Stony Brook University

Validating the use of fluorescent proteins as molecular probes in vivo and in vitro

A Thesis Presented

by

Laura Elizabeth Dougherty

to

The Graduate School

in Partial Fulfillment of the

Requirements

for the Degree of

Master of Science

in

Biochemistry and Cell Biology

Stony Brook University

December 2014

Stony Brook University

The Graduate School

Laura Elizabeth Dougherty

We, the thesis committee for the above candidate for the

Master of Science degree, hereby recommend

acceptance of this thesis.

Mark Bowen-Thesis Advisor
Associate Professor, Department of Physiology and Biophysics

Suzanne Scarlata-Second Reader
Professor, Department of Physiology and Biophysics

This thesis is accepted by the Graduate School

Charles Taber
Dean of the Graduate School

Abstract of the Thesis

Validating the use of fluorescent proteins as molecular probes in vivo and in vitro

by

Laura Elizabeth Dougherty

Master of Science

in

Biochemistry and Cell Biology

Stony Brook University

2014

Fluorescent proteins are widely used in cell biology as molecular probes to observe a protein of interests location and movement and also to study protein-protein interactions. The study of protein-protein interactions is observed using a technique called fluorescent resonance energy transfer (FRET). FRET is used as a way to approximate distances between proteins in vivo and requires at least two fluorescent proteins in order to utilize the process. The most popular pairing is enhanced cyan and yellow fluorescent (eCFP/eYFP) proteins. To view protein localization, fluorescent proteins are attached to the protein of interest. PSD-95, a scaffolding protein in the post synaptic density of neurons has been studied with the use of fluorescent protein tags. PSD-95 is made up of three PDZ domains attached to an SH3 and GK domain by an intrinsically disordered linker. Specific interactions between the SH3 and GK domain must occur for PSD-95 to fold properly.

This study has two objectives. The first objective is to create an in vivo FRET fluorescent protein reference ruler. To accomplish this, a series of eCFP/eYFP tandems were created with

three different linker lengths to characterize their FRET interactions in vitro and in vivo. The results show that in vitro measurements are 4 times larger than in vivo measurements, however, they follow a similar trend. The second objective of this study sets out to see if folding the SH3-GK domain of PSD-95 is altered by the addition of a C-terminal fluorescent protein tag and to see how the fluorescent protein localize relative to PSD-95. A construct containing the SH3-GK of PSD-95 attached to eYFP by a 5 residue linker was created with cysteine labeling sites to observe intramolecular interactions between the SH3 and GK domains and intermolecular interactions between the SH3-GK domain and eYFP. Interactions were characterized using smFRET and compared to previously reported data of the SH3-GK domain in the absence of eYFP. Results suggest that eYFP does not affect the folding of the SH3-GK domain of PSD-95.

Table of Contents

List of Figures

List of Tables

List of Abbreviations

FP	fluorescent protein
GFP	green fluorescent protein
eYFP	enhanced yellow fluorescent protein
eCFP	enhanced cyan fluorescent protein
eGFP	enhanced green fluorescent protein
FRET	Fluorescent resonance energy transfer
E	FRET efficiency
I_D	Donor intensity
I_A	Acceptor intensity
r	Distance between fluorophores
R_o	Föster's radius
CLY	enhanced cyan fluorescent protein-linker-enhanced yellow fluorescent protein
PSD-95	post synaptic density protein 95
MAGUK	membrane associated guanylate kinase
SH3	SRC homology 3
GK	guanylate kinase
PFP	SH3-GK domain of PSD-95 attached to eYFP
PCR	polymerase chain reaction
TIRF	total internal reflection
smFRET	single molecule fluorescent resonance energy transfer
MW	molecular weight
A	anisotropy
E_{obs}	proximity ratio
kDa	kilo Daltons
SDS PAGE	sodium dodecyl sulfate polyacrylamide gel electrophoresis
NaCl	sodium chloride
TB	Terrific broth
IPTG	Isopropyl β-D-1-thiogalactopyranoside
SEC	size exclusion chromatography
R_H	hydrodynamic radius
Ve	elution volume
Å	Angstroms
Vi	initial volume
Vo	void volume
M_r	apparent molecular weight
CHO	Chinese hamster ovary

Acknowledgments

I would like to thank Professor Bowen for allowing me to join his lab and being an outstanding mentor. Without his guidance this thesis would not have been possible.

I would also like to thank Dr. Scarlata for taking the time to be my second reading and giving me valuable feedback on my thesis.

1. Introduction

Fluorescent proteins (FPs) are widely used in cell biology as molecular probes in mammalian, plant and bacterial cells [1] [2]. In 1962, green fluorescent protein (GFP) was extracted and purified from *Aequorea victoria*, a jelly fish found off the pacific coast [3]. Green fluorescent protein forms an 11 stranded beta sheet barrel with a coaxial helix in the center containing a serine-tyrosine-glycine chromophore [4]. During protein folding the chromophore center under goes a cyclization and oxidation reaction to fluoresce [5]. Misfolding of the protein, results in no chromophore formation [6].

Variants of GFP have been created by amino acid substitutions, expanding spectral range [7]. Examples include enhanced yellow fluorescent protein (eYFP), enhanced cyan fluorescent protein (eCFP) and blue fluorescent protein [8-10]. Besides spectral differences, variants also have different photophysical properties. Enhanced GFP (eGFP) has 6-fold greater brightness compared to wild type GFP [11]. Venus is an improved version of eYFP, exhibiting improved folding and reduced pH sensitivity [12].

Fluorescent proteins are used in cellular biology to visualize localization, movement and turnover rates of proteins of interest [13]. Fluorescent proteins are attached to proteins of interest at the amino (N) or carboxyl (C) terminus by a peptide linker, allowing protein movements to be characterized in vitro and in vivo. The creation of GFP variants have allowed for protein-protein interactions and conformational changes to be studied and has given researchers the ability to visualize multiple cell structures at the same time though multicolor imaging [14]. Protein-protein interactions and conformational changes can be characterized by fluorescent resonance energy transfer (FRET) to approximate distances between proteins [15].

In FRET, FPs are used to monitor protein-protein interactions and conformational changes. Two different FPs are used as donor and acceptor. There is direct excitation of the donor FP causing it to go to high energy state. As the donor returns back to ground state, it interacts with the acceptor though a dipole-dipole interaction and transfers energy. The emission intensities of donor (I_D) and acceptor (I_A) are used to calculate FRET efficiency (E).

$$E = \left(\frac{I_A}{I_A + I_D}\right) \qquad (1)$$

The FRET efficiency can then be used to calculate the distance between proteins.

$$FRET = \frac{1}{1+\left(\frac{r}{R_0}\right)^6} \qquad (2)$$

Where *FRET* is the FRET efficiency, r is the distance between fluorophores and R_o is Föster's radius, which includes the photophysical parameters for FRET to occur [16]. Those parameters include spectral overlap of donor emission and acceptor excitation, distance between FPs and relative orientation of the FPs (Figure 2) [17] . The donor quantum yield is also included in R_o. The quantum yield is the amount of photons emitted relative to the amount of photons absorbed. Higher quantum yield means increased brightness. There are multiple ways to calculate FRET efficiency which may be referred to as the proximity ratio or observed FRET efficiency, however, the formula (Eq. 2) to calculate distance remains the same.

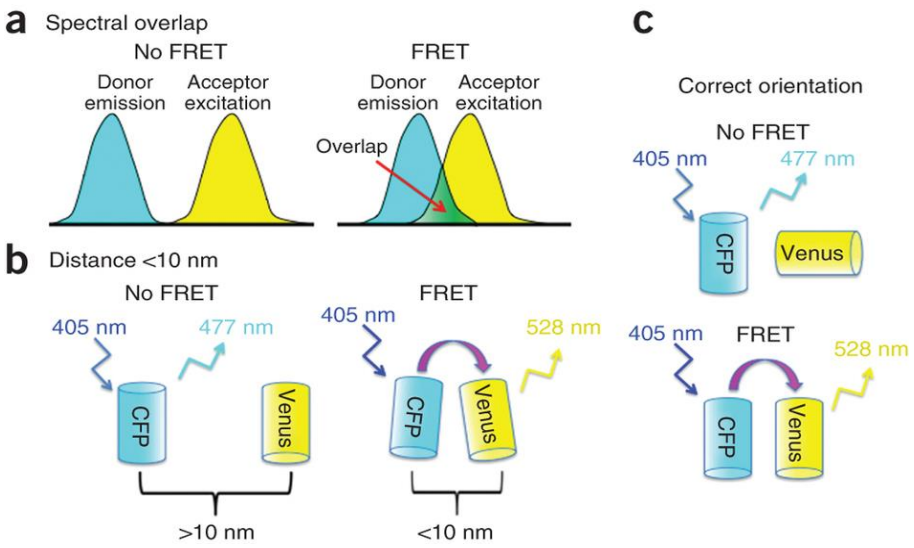

Figure 1. Conditions for FRET to occur: a. the donor emission must overlap the acceptor excitation in order for the donor to transfer energy to the acceptor. b. distance between FPs must be closer than 10nm for transfer to occur. c. For dipole-dipole interactions to occur FPs must be in a correct orientation relative to each other. Figure adapted from Broussard et al. [18]

The most common FP pair used in FRET is eCFP and eYFP where eCFP is the donor and eYFP is the acceptor. Ideally, the relative brightness of eCFP and eYFP should be similar, however, eYFP is 5 times brighter than eCFP. Enhanced cyan fluorescent protein has a quantum yield of 37% and eYFP has a quantum yield of 61% [19]. Although spectral overlap is needed for FRET to occur, the donor channel can leak into the acceptor channel and cross talk between the donor and acceptor can occur (Figure 2) [20]. To correct for overlap and leakage, the individual spectra of the donor and acceptor must be known. Despite limitations with FP FRET, it is the only way to view protein-protein interactions and conformational changes in vivo.

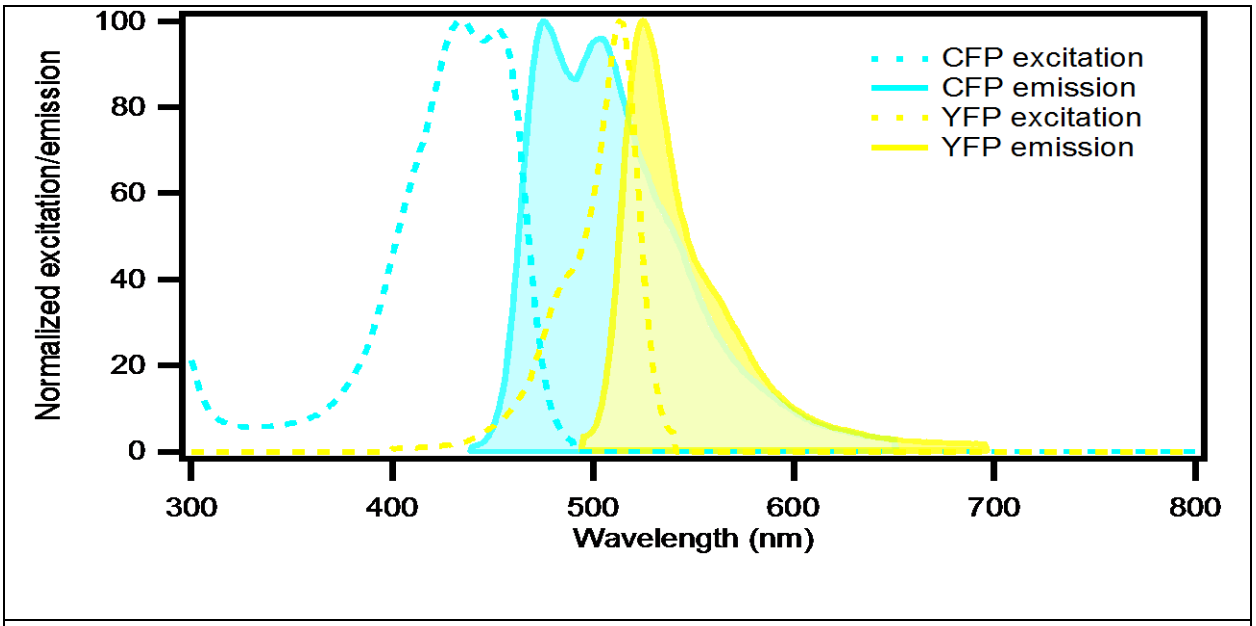

Figure 2: Excitation and emission spectra of eCPF and eYFP. The blue dashed line and shaded area represent eCFP excitation and emission. The yellow dashed line and shaded area represent eYFP excitation and emission spectra. Leakage is where the eCFP and eYFP emission overlap, shown as a pale tan color. Cross talk is the direct excitation of eYFP during the excitation of eCFP.

To characterize interactions between eCFP and eYFP in vitro and in vivo a series of CFP/YFP tandems (CLYs) were created with three different linker lengths. Interactions were characterized in vitro using ensemble fluorescence microscopy and the proximity ratios were also calculated. To characterize interactions in vivo, CLYs were transfected into Chinese hamster ovary (CHO) cells and the proximity ratios were calculated. In vitro and in vivo results were compared. Using size exclusion chromatography (SEC) the apparent molecular weight (M_r) and the hydrodynamic radius (R_H) of the CLYs were calculated to estimate the apparent size of the proteins. Ultimately a reference ladder will be created for in vivo FRET measurements.

Fluorescent protein tags are attached to proteins of interest to study localization and movement. One protein that has been studied with FP tags is PSD-95, which is located in the post synaptic density of neurons. PSD-95 is a scaffolding protein that helps organize glutamate

receptors and signal pathways [21, 22]. A member of the MAGUK family, PSD-95 is made up of three PDZ domains attached to a SRC homology 3 (SH3) and guanylate kinase (GK) domain by an intrinsically disordered linker. Previous studies have attached FPs to PSD-95 in vivo to monitor its localization and movement. However, the effects of attachment have not been characterized [23].Studies have shown that the SH3 and GK domain of PSD-95 interact with each other for proper protein folding to occur [24]. Does the attachment of a FP affect the folding of SH3-GK domain or interfere with normal protein function? To address these questions, the SH3-GK domain of PSD-95 has been attached to eGFP and eYFP by a short linker (Figure 3). The PSD-95 and FP constructs will be referred to as PFPs. Labeling sites have been introduced to observe intramolecular interactions between the SH3 and GK domains of PSD-95 and intermolecular interactions between the SH3-GK domain and eYFP using single molecule FRET. Intramolecular interactions with eYFP attached were compared to previously made measurements in the absence of eYFP [25].

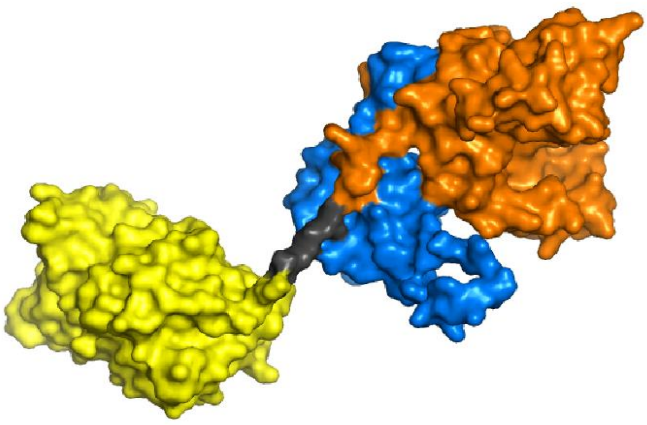

Figure 3: A surface model of the PFP construct. The SH3 and GK domains of PSD-95 are blue and orange, respectively. The residue is black and eYFP is yellow. The formula molecular weights of eYFP and the SH3-GK domain of PSD-95 are approximately 30 and 36 kDa respectively.

2. Materials and Methods

2.1 Construct assembly:

Single FPs were PCR amplified from existing constructs and ligated into pET28-a (Novagen, Madison, WI), or PROEX-HTB (Invitrogen, Carlsbad, CA) vectors containing a N-terminus 6-histidine tag. The CLY constructs were a generous gift from the Merkx lab [26]. Additional CLYs were constructed by substituting Venus for eYFP (Table 1).

CLY Constructs	Linker length	2nd FP
CLY 1	23	eYFP
CLY 1B	23	Venus
CLY 5	47	eYFP
CLY 5B	47	Venus
CLY 9	71	eYFP

Table 1: CLY constructs with linker length and second fluorescent protein. Additional constructs with 23 and 47 residue linkers' were made by substituting Venus for eYFP. Enhanced cyan fluorescent protein is always the first FP. The linker is considered last 13 residues in the eCFP sequence followed by GGSGGS repeats and the first 4 residues in eYFP [26]. The CLY construct number refers to the number of GGSGGS repeats present.

A construct containing full length PSD-95 in a eGFP mammalian expression vector was a gift from David Bredt [22]. The SH3-GK domains of PSD-95 attached to eGFP were cloned out of the mammalian vector and cloned into a prokaryotic expression vector. The SH3-GK domain was then cloned out of the prokaryotic vector and inserted in the CLY 1 construct between the eCFP and eYFP. The SH3-GK domain and eYFP section of the CLY was cloned into another prokaryotic expression vector. This construct of the SH3-GK domain and eYFP (referred to as the PFP construct) was used for further study. Quikchange® site directed mutagenesis (Agilent Technologies, Santa Clara, CA) was used to knock out the chromophore of eYFP and remove the

two native cysteines at residues 46 (C46S) and 71 (C71M). Once removed, new cysteine sites were introduced as labeling sites (Figure 4).

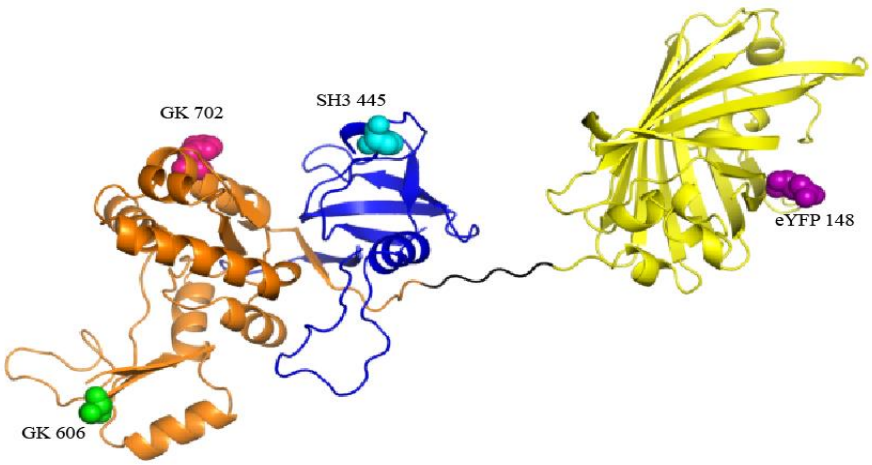

Figure 4: The PFP construct with labeling sites identified. The SH3 domain is shown in blue with the 445aa labeling site shown as cyan. The GK domain is orange with the 606aa and 702aa labeling sites shown as green and pink respectively. The eYFP is shown as yellow with the 148aa site shown in purple. The linker is shown in black connecting the GK domain to eYFP.

2.2 Protein expression:

All constructs were transfected into the Rosetta *E. coli* (Novagen, Billerica, MA) following manufacturers protocol. Growths were carried out in TB media. Single FPs and CLYs induction was carried out at 30°C with 0.5mM IPTG (Isopropyl β-D-1-thiogalactopyranoside) for three hours. Induction of the PFPs was carried out at 25°C with 0.1mM IPTG.

2.3 Protein Purification:

Purification of all proteins was completed using nickel affinity and anion exchange chromatography in the presence of reducing agents. PFPs were further purified by size exclusion

chromatography on a Superdex 200 GL column (GE Healthcare). Sample purity were observed by 12% SDS-PAGE (Figure 10).

2.4 Analytical size exclusion chromatography (SEC) and Hydrodynamic radius (R_H):

Single FP and CLY samples were run on a Shodex KW-800 analytical column (Showa Denko America Inc., New York, NY). To determine apparent molecular weight, (M_r) known standards thyroglobulin, Y-globulin, ovalbumin, myoglobin and vitamin B-12, were run. A standard curve was created based on the log of their molecular weights and their elution volume (*Ve*):

$$Ve = Vi - Vo \qquad (3)$$

Where *Vi* is the initial elution volume and *Vo* is the column void volume. For the Shodex KW-800 analytical column the void volume is 6 mL. The equation of the line obtained from the standard curve was used to then determine the M_r of single FPs and CLYs. Using the M_r, the hydrodynamic radius was calculated as previously described [27].

$$R_{H=(-0.204+0.357*LOG\ (M_r))} \qquad (4)$$

2.5 Ensemble fluorescence:

Ensemble fluorescence spectra measurements were made on an ISS PCI photon counting spectrofluorimeter with a 10 mm excitation slit and a 5 mm emission slit. Single fluorescent proteins and CLYs were diluted to 0.05 absorbance at 458 nm. Samples were excited at 458 nm and emission spectra were collected from 463-749 nm. Samples were then excited at 514 nm and emission spectra data were collected from 519-749 nm. Anisotropy measurements were collected

using Glan Thompson polarizers in the L conformation with samples excited at 458 nm with data collected at 476 nm.

2.6 Calculation of FRET:

Emission data collected from the fluorimeter was used to calculate the proximity ratio. Emission spectra from eCFP alone and the CLYs was normalized to 475 nm. The proximity ratio (*E*) for the CLYs was calculated as:

$$E = \frac{A}{D+A} \qquad (5)$$

Where *A* is the sum of the normalized CLY intensities and *D* is the sum of the normalized eCFP intensities from 463- 750 nm. To calculate the distance between chromophores (*r*) the proximity ratio (*E*) and R_o values were used. The R_o value used for the CLYs is 48Å, as previously calculated by Evers et al [26].

$$r = R_0 \left(\frac{1}{E} - 1\right)^{1/6} \qquad (6)$$

2.7 Live cell FRET:

CLY samples 1, 5, and 9 were transfected into CHO cells plasma membrane (Figure 5). Enhanced CFP and eYFP were also transfected into cells as well for control samples.

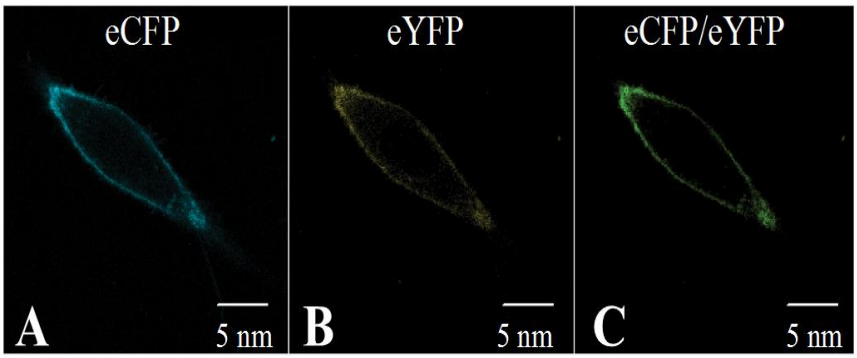

Figure 5: Live cell images of CLYs in CHO cells. CLY constructs were attached to a protein targeting the plasma membrane. A. eCFP is excited at 458 nm B. eYFP is excited at 514 nm. C. an overlay of eCFP and eYFP when FRET occurs.

Using a Nikon Eclipse Ti-S microscope with a 3 cube filter set, emission spectra data was collected by an iXon camera (Andor technologies, Belfast, UK). The 3 cube filters used were Zeiss filter set 51 for measurement of eCFP, Zeiss filter set 53 for measurement of eYFP and Chroma 458/514 dual band that measures both eCFP and eYFP emission spectra. The proximity ratio was then calculated (Eq. 5). The donor "D" was calculated as the CLY emission from the Ziess filter set 51 (*cfp*) , eCFP emission from the Chroma 458/514 dual band (*458tirf*) and eCFP emission from the Ziess filter set 51 (*cfp*).

$$D = \mathrm{CLY}(cfp) \times \frac{\mathrm{eCFP}(458tirf)}{\mathrm{eCFP}(cfp)} \qquad (7)$$

The acceptor "A" was calculated as CLY emission from the Chroma dual band (*458tirf*), CLY emission from the Chroma dual band (*514tirf*), the ratio of eYFP from the Chroma dual band (*458tirf/51tirf*) and donor. Using the ratio of eYFP at the donor and acceptor excitation wavelengths corrects for eYFP crosstalk and using the eCFP emission at 514 nm corrects for eCFP leakage.

$$A = \mathrm{CLY}(458tirf) - \left[\mathrm{CLY}(514tirf) \times \left(\frac{\mathrm{YFP}(458tirf)}{\mathrm{YFP}(514tirf)}\right)\right] - D \qquad (8)$$

2.8 PFP Labeling and encapsulation:

Purified PFP samples were labeled with a mixture of maleimide derivatives dyes, Alexa 555 and Alexa 647, (Invitrogen, Carlsbad, CA) overnight. Free dye was removed from labeled proteins by desalting Sephadex G-50 (GE Healthcare). Labeled PFP samples were encapsulated into 100nm liposomes composed of egg phosphatidylcholine with 0.1% biotinylated phosphatidylethanolamine (Avanti Polar Lipids, Alabaster, AL) by extrusion. Encapsulated samples were separated from freely diffusing proteins by desalting on Sepharose CL-4B columns (GE Healthcare).

2.9 Single molecule FRET (smFRET):

Quartz slides were prepared for single molecule measurements on a prism-type total internal reflection (TIRF) microscope with a layer of 1 mg/mL biotinylated bovine serum albumin (BSA), followed by 0.1 mg/mL streptavidin. Labeled, encapsulated PFP samples were then added to the quartz slide in concentrations sufficient to observe single molecules. Oxygen scavenging system and triplet state quenchers were added to delay bleaching and prevent dye blinking. Data was collected with an iXon EMCCD camera (Andor Technologies, Belfast, UK) running at 100 ms/frame.

Data was analyzed with MATLAB software (Mathworks, Natik, MA). Single molecules were selected based on the presence of a single donor and acceptor dye, with anti-correlated photobleaching. Selected traces were then viewed with IGOR Pro (Wavemetrics, Portland, OR) and observed single molecule FRET efficiency (smFRET) was calculated as:

$$smFRET = \frac{I_A}{I_A + \gamma I_D}. \qquad (9)$$

where "I_A" is the acceptor intensity and "I_D" is the donor intensity. The "γ" is a normalization factor, correcting for differences in quantum yield and detection efficiencies of dyes [16]. Using the FRET efficiency, the distance between fluorophores can be calculated as:

$$r = R_{o*}\left(\frac{1}{smFRET} - 1\right)^{1/6} \qquad (10)$$

Where *r* is the distance (Å) between fluorophores and R_o is Föster's radius. The R_o value of the Alexa 555 and 647 dyes provided by the manufacturer is 51. However, when the dyes are attached to proteins their quantum yield (*Qy*) changes. To account for these changes a new R_o value known as R_{o*} was used to calculate distance using the observed *Qy* , given *Qy* (.01) and R_o (51) of Alexa 555 and 647.

$$R_{o*} = 51\left(\frac{Qy}{0.1}\right)^{1/6} \qquad (11)$$

The resulting distances were compared to previously calculated distances by McCann et al [25].

3. Results

3.1 Analytical SEC and Hydrodynamic radius (R_H) of single FPs and CLYs:

The hydrodynamic radius and apparent size of a protein depends on it's M_r. The formula weight of the single FPs and CLYs were determined from sequencing data (Table 2), and M_r were viewed by 12% SDS PAGE (Figure 6). To determine the M_r of the CLYs and single FPs in solution, SEC was used. Single FPs were first run on a Shodex KW-800 analytical column to find a condition where their elution volumes were similar. The single FPs have similar formula weights and should run at very similar elution volumes on the column. Once a condition was

found where the single FPs elution volumes were similar, the CLY samples were run in the same conditions.

Single FP	Formula MW	CLY tandems eCFP-eYFP	Formula MW	CLY tandems eCFP-Venus	Formula MW
eCFP	29.3	**CLY 1**	57.0	**CLY 1B**	56.9
eYFP	30.5	**CLY 5**	58.7	**CLY 5B**	58.5
Venus	30.3	**CLY 9**	60.1		

Table 2: The calculated molecular weight (MW) of single FPs and CLYs based on sequencing data. All weights are shown in kDa

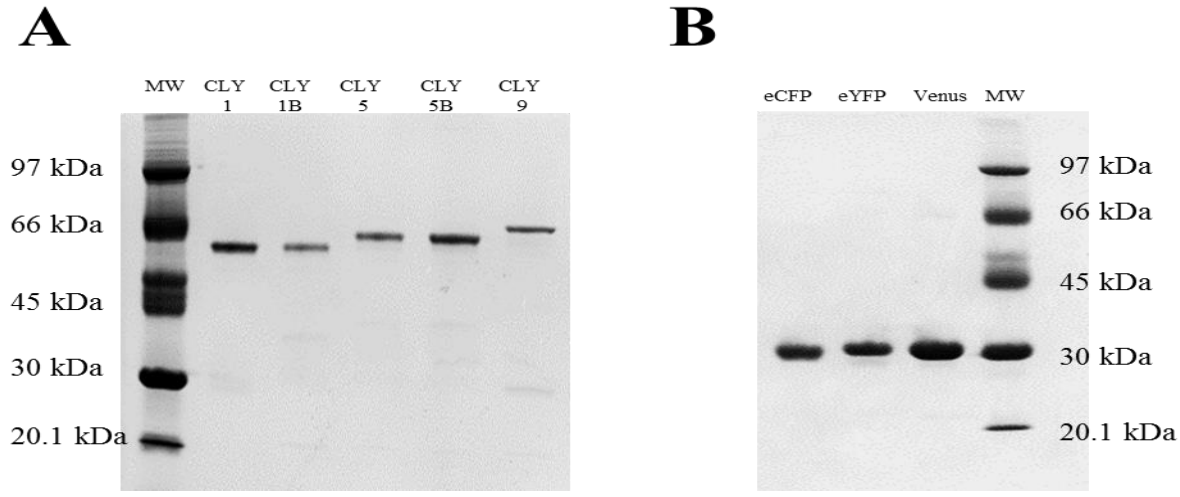

Figure 6: 12% SDS PAGE of CLY and single FP samples. A. shows the standard molecular weight ladder (MW) and the CLY samples from CLY 1-CLY 9. B shows the single FPs, eCFP, eYFP and Venus. CLY size increases as linker length increases. Single FPs are all similar sizes.

The first condition screened was salt concentration (Table 3). High salt is commonly used to prevent non-specific interactions of the proteins with the SEC column. Using a 20mM tris buffer solution at pH 7.5 single FPs were run in 300mM NaCl and 500mM NaCl. At 300mM NaCl the single FPs had different elution volumes, resulting in different apparent molecular

weights that were not near formula weights. At 500mM salt the proteins had increased retention volume, indicating that the proteins were interacting with the beads. In an attempt to decrease bead interactions 0.1% thesit was added to the 300mM NaCl solution. This decreased the elution volume of eYFP and Venus, however eCFP showed little change. In high salt concentrations the single FPs did not have the similar elution volumes due to interactions with the beads.

	Elution volume (Ve)		
Sample	**300mM NaCl**	**500mM NaCl**	**300mM NaCl + .1% thesit**
eCFP	3.06	-	2.96
eYFP	2.67	3.62	2.47
Venus	2.98	3.66	2.39

Table 3: Single FPs run in different salt (NaCl) conditions in 20mM tris pH 7.5. The elution volumes, in milliliters, vary between single FPs and salt concentrations. In 500 mM NaCl eYFP and Venus had similar elution volumes but their M_r were only 11.5 kDa. The addition of .1% thesit reduced elution volumes of eYFP and Venus, but not eCFP.

The second condition screened was pH. At pH 7.5, all the single FPs are negatively charged, however at pH 6.5 eCFP has a neutral charge while eYFP and Venus are negatively charged. Using a low salt concentration (100mM) single FPs were run in a 50mM sodium phosphate buffer, pH 6.5. At the lower pH both eYFP and Venus had similar elution volumes of 2.29 mL and 2.27 mL respectively while eCFP was retained in the column longer eluting at 2.9 mL.

The high salt conditions and low pH condition did not resolve the differences in single FP elution volumes. A 50mM HEPES buffer was used with low salt (100mM NaCl), and pH 7.4. Returning to a higher pH all single FPs were negatively charged, and a lower salt concentration reduced elution volumes and bead interactions. During the first run the elution volume of eCFP

decreased compared to previous conditions but still not near eYFP or Venus; however, the elution volumes of eYFP and Venus remained similar to each other. To insure that the single FPs were not interacting with beads 1M urea was added to the buffer and the proteins were run again. The addition of 1M urea did not have a large effect on the elution volumes (Table 4).

All the single FPs were expressed with a 6-his N terminus tag for nickel purification. To see if the 6-his tags were affecting the elution volumes of the single FPs, they were cleaved off with proteases and then run again in the 100mM, 7.4 pH 50mM HEPES buffer. The removal of the 6-his tag reduced the retention volume of eCFP and it now had an elution volume similar to eYFP and Venus (Table 4). To see if the removal of the 6-his tag affected the eCFP elution volume in high salt, it was run again with the 300mM NaCl, 20mM tris at pH 7.5 buffer. The elution volume with and without the 6-his tag was 3.06 mL and 3.05 mL respectively.

	Elution Volume (Ve)			M_r
Sample	**100 mM NaCl**	**100 mM NaCl + 1 M urea**	**100 mM NaCl No 6-his tag**	**100 mM NaCl No 6-his tag**
eCFP	2.70	2.57	2.48	40.0
eYFP	2.47	2.35	2.35	46.0
Venus	2.43	2.42	2.36	45.5

Table 4: Elution volumes (mL) of single FPs in 50mM HEPES pH 7.4, Low salt (100 mM). The addition of 1M urea reduced the elution volume of eCFP and eYFP. The removal of the 6-his tag led to similar elution volumes of the single FPs with a .13 range difference. Using the elution volumes from the 6-his tag removal the M_r of the single FPs was calculated.

The single FPs in 100mM NaCl, pH 7.4 in 50mM HEPES with removed 6-his tags gave the most similar elution volumes. The CLYs were run in the same conditions with their 6-his tags removed. The elution volumes CLY 1 and 1B were similar and had the largest elution

volumes, followed by CLY 5 and 5B then CLY 9. Using the elution volumes from the CLYs in the low salt HEPES buffer, the apparent molecular weights were calculated and then used to determine their hydrodynamic radii (Table 6). The hydrodynamic radius of the CLYs increased as the linker length increased.

Sample	Ve	M_r	R_H
CLY 1	1.6	94.3	37.3
CLY 1B	1.58	96.3	37.6
CLY 5	1.50	104.6	38.7
CLY 5B	1.48	106.8	39.0
CLY 9	1.40	114.8	40.0

Table 5: Analytical SEC of CLYs in 100mM NaCl in a 50mM HEPES 7.4 pH buffer. The elution volumes (Ve), in milliliters, was used with the standard curve to calculate the apparent molecular weight (Mr) of the CLYs shown in kDa. Using the M_r the hydrodynamic radius (R_H) was calculated in nm.

3.2 Ensemble Fluorescence and in vivo Measurements of CLYs:

The proximity ratios and *r* apparent values were calculated for CLYs 1, 5 and 9 using ensemble fluorescence. Results were compared to previously reported data by Evers et al. (Table 6) [26]. To calculate the proximity ratio (E_{obs}) as described by Evers et al.:

$$E_{\text{obs}} = \frac{\epsilon_{\text{A}}(\lambda_{\text{D}}^{\text{ex}})}{\epsilon_{\text{D}}(\lambda_{\text{D}}^{\text{ex}})}\left[\frac{F_{\text{AD}}(\lambda_{\text{A}}^{\text{em}})}{F_{\text{A}}(\lambda_{\text{A}}^{\text{em}})} - 1\right] \quad (12)$$

the extinction coefficients of eYFP (ϵ_A) and eCFP (ϵ_D) at eCFP excitation wavelength (λ_D^{ex}) were used. Using their formula, our proximity ratios for CLY 1, 5 and 9 were only 0.2, 0.18 and 0.16 respectively. Our calculations were then done as described in the methods to obtain suitable values.

	Our Calculations			Evers et al. calculations		
Sample	*FE*	*A*	*r (Å)*	*FE*	*A*	*r (Å)*
CLY 1	0.83	0.349	36.8	0.71	0.370	41.3
CLY 5	0.74	0.345	40.6	0.56	0.350	46.1
CLY 9	0.71	0.343	41.5	0.43	0.332	50.3

Table 6: Fluorescence ensemble FRET efficiency (FE), anisotropy (A) and distance (r) in angstroms was calculated for CLYs 1, 5, and 9. Calculations of CLYs FE, A and r were previously calculated by Evers et al **[26]**.

The proximity ratio of the CLYs was measured in vivo were compared to our CLYs measured in vitro. Using the R_H value obtained from SEC, the proximity ratios were compared, showing similar trends in slope (Figure 7).

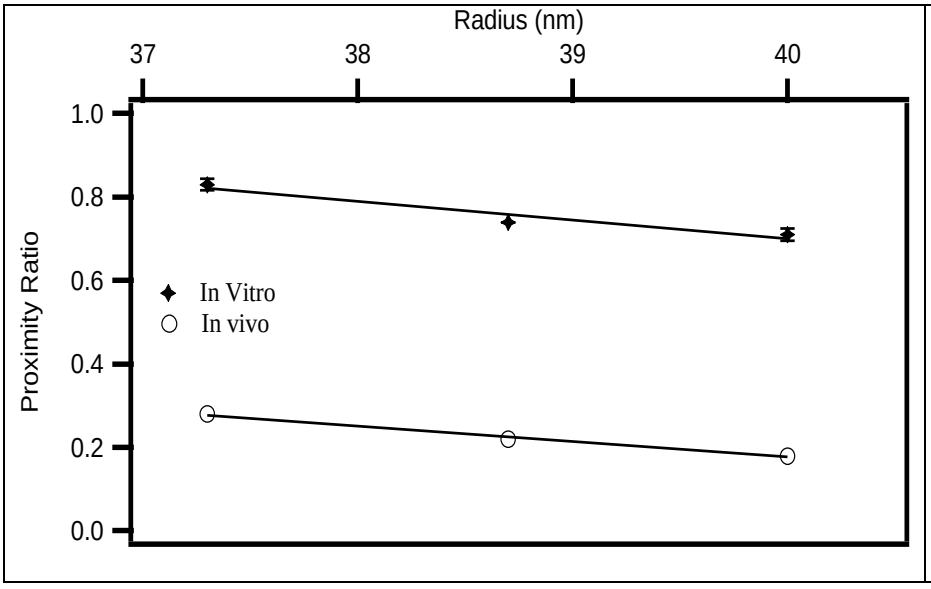

Figure 7: The proximity ratios in vitro and in vivo compared to the hydrodynamic radius calculated from SEC measurements. The slopes of each graph similar with -0.04 and -0.037 for in vitro and in vivo respectively. Although the proximity ratios in vitro are 4 times larger than in vivo they have similar trends. Error bars for in vitro measurements based of standard deviation of duplicate samples.

3.3 Expression of PFPs:

The original PFP construct before mutations knocked out the chromophore of eYFP was highly soluble (Figure 10). Once eYFP mutations were introduced, analysis of lysis and soluble PFP fractions showed that a majority of the desired protein was insoluble. Growth conditions were then modified in an effort to obtain more soluble protein. Modifications included lowering the induction temperature from 30°C to 25°C and reducing the amount of IPTG added from 0.5mM to 0.1mM. These modifications resulted in more soluble proteins (Figure 8).

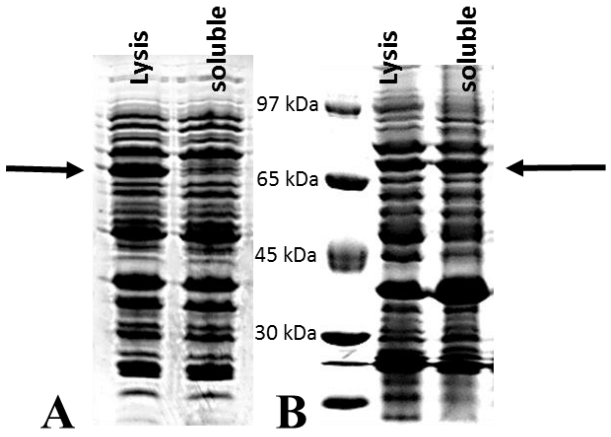

Figure 8: PFP 1 lysis and soluble fractions, the arrow indicates the desired band. A. Induction preformed at 30°C shows most of the desired product is insoluble. B. Induction preformed at 25°C increased solubility of the protein.

3.4 Purification of PFPs:

Initial elutions following nickel affinity chromatography showed very low purity with multiple contaminants including degradation products. To reduce contaminants, wash buffers containing varying imidazole concentrations were screened. A 50mM wash greatly reduced secondary bands and was used on all purifications afterwards (Figure 9).

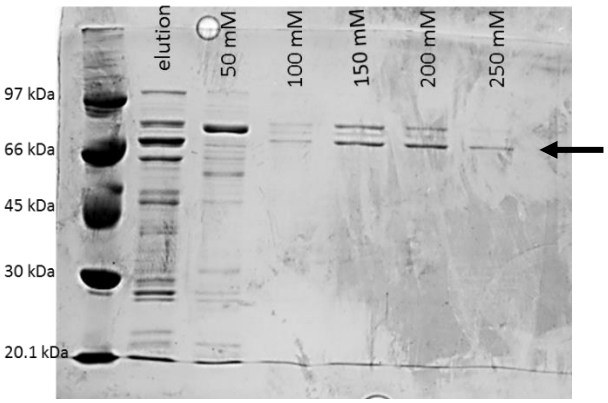

Figure 9: Imidazole screening of elutions after nickel affinity purification. Lane 1 is the molecular weight ladder. Lane 2 is initial elution after nickel affinity purification. Lane 3-7 are the elutions from different concentrations of imidazole washes increasing from 50mM- 250mM. The arrow indicates the PFP protein. At a 50mM wash, most contaminants are eluted

Anion affinity chromatography was used to further purify the PFPs removing more contaminants but, it also reduced protein yield. Further investigation showed that PFPs were interacting with the column beads resulting in lower yields. Size exclusion chromatography was used for final purification. Samples showed increased purity with no contamination bands visible on 12% SDS-PAGE. However, as seen with anion exchange, sample yield in size exclusion was reduced as a result of PFPs interacting with the column beads.

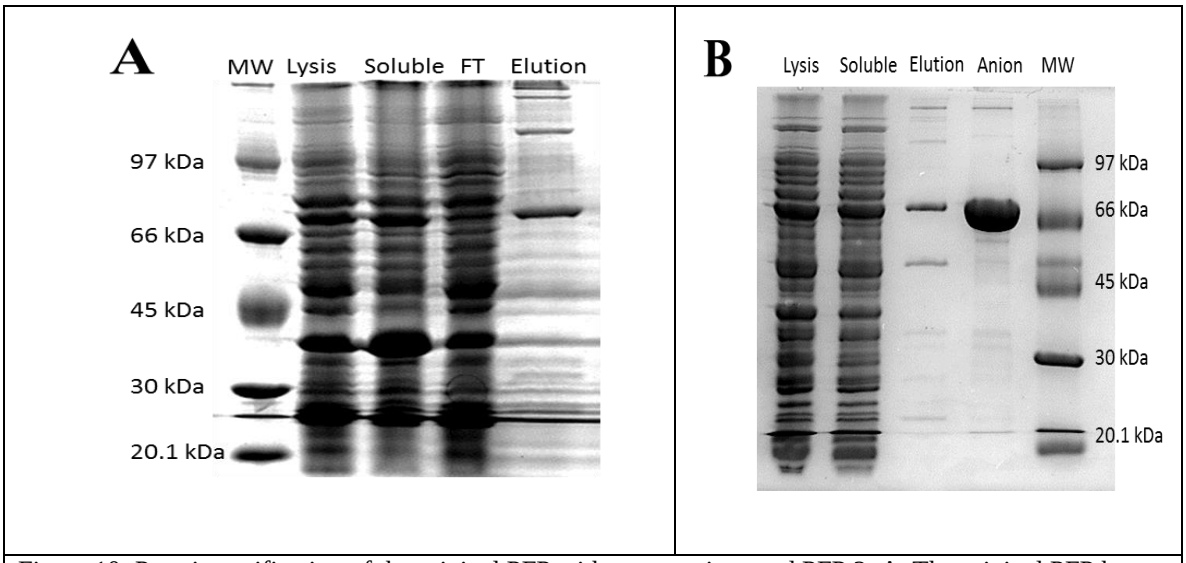

Figure 10: Protein purification of the original PFP with no mutations and PFP 2. A. The original PFP has little contaminants in the elution and after anion the majority of secondary bands are removed. B. PFP 2 shows more contaminants in the elution. The FT is the flow through after incubation with the nickel beads.

3.5 Single molecule FRET (smFRET):

Double labeled PFP traces were analyzed for anti-correlation between acceptor and donor dyes. FRET traces were selected and FRET efficiency was calculated (Figure 11). For each sample over 150 traces were selected.

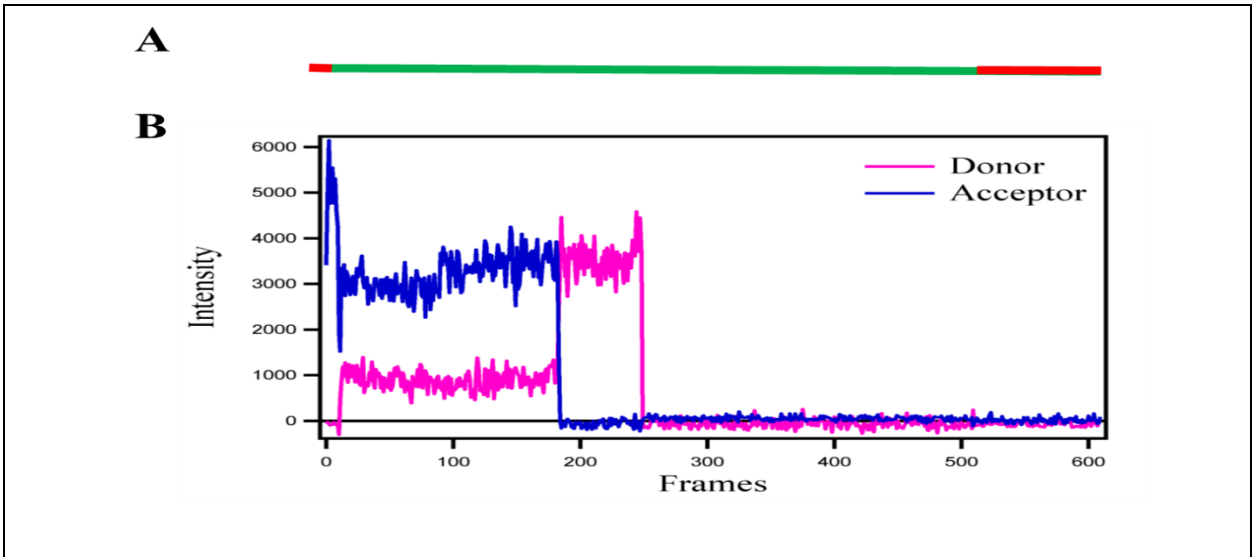

Figure 11: Select trace file from PFP 1 measurements. A. The different laser colors, red and green represent 633 nm and 532 nm respectively. B. Example of a FRET trace where there is anti-correlated photo bleaching.

The FRET efficiency and distances between fluorophores of PFP 1 and 2 contain labeling sites in the SH3-GK domain and were compared to previous measured sites in PSD-95 alone (Figure 12) [25]. PFP 1 and PSD-1 each contain labeling sites on residue 445 in the SH3 domain and 606 in the GK domain. PFP 1 had a FRET efficiency of 0.32 and distance of 63.2 Å, while PSD-1 had a FRET efficiency of 0.325 and a distance of 62.9 Å. Although the values are not exactly the same, they do not indicate any major differences in folding with and without eYFP attached. PFP 2 and PSD-19 contain labeling sites at residue 445 in the SH3 domain and 702 in the GK domain. PFP 2 had a FRET efficiency of 0.743 and a distance of 49.8Å and PSD-19 had a FRET efficiency of 0.782 and a distance of 48 Å. The distances between PFP 2 and PSD-19 differ by 1.8Å.

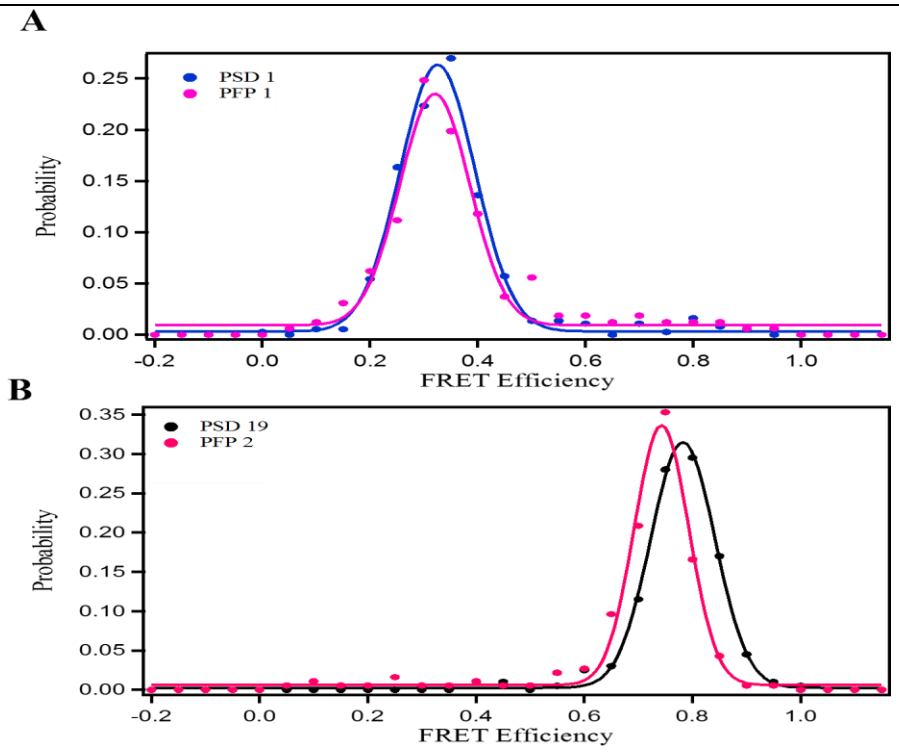

Figure 12: FRET efficiency and curve fitting. A. PFP 1 and PSD 1 are fitted to Gaussian curves. B. PFP 2 and PSD 19 are fitted to Gaussian curves. The peak of the graph is the FRET efficiency. The PSD-95 samples differ from their reported values by McCann et al, as they were recalculated the same way as the PFPs.

The FRET efficiency was calculated for PFP 3, containing a labeling site at residue 148 in eYFP and at residue 445 in the SH3 domain of PSD-95. Traces were fit to a Gaussian curve. The FRET efficiency calculated was 0.5625 (Figure 13). PFP 3 does not fit the Gaussian curve as well as PFP 1 and 2. The width of the PFP 3 curve is 0.36, while PFP 1 and 2 are 0.071 and 0.098 respectively.

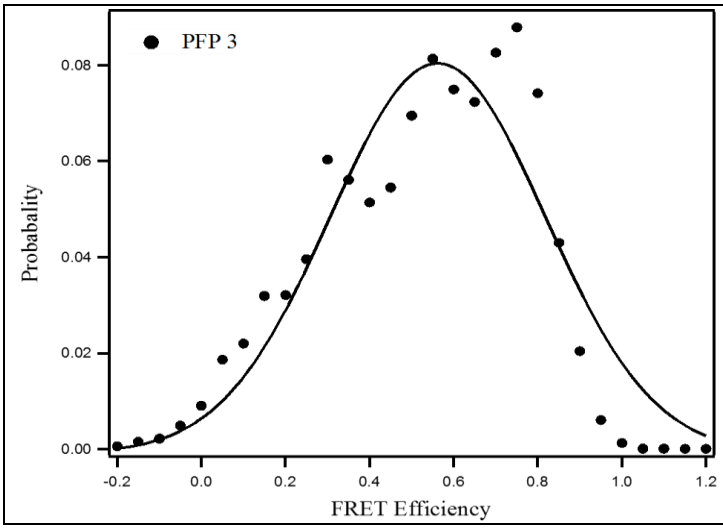

Figure 13: FRET efficiency of PFP 3 fit to a Gaussian curve. PFP 3 does not fit well and has a very board peak of 0.36. At the peak of the Gaussian curve the FRET efficiency is 0.5625.

4. Discussion:

Fluorescent Proteins are widely used in cell biology as molecular probes. Fluorescent proteins are attached to proteins of interest and allow observation of localization and movement. One study completed by Craven et al used full length PSD-95 attached to eGFP in hippocampal neuron cells to observe post synaptic clustering [28].

The creation of GFP variants are used to characterize protein-protein interactions and conformational changes in vivo and in vitro. A commonly used pair of FPs are eCFP and eYFP. Using single molecule FRET and ensemble fluorescence FRET, distances between proteins and conformational changes can be characterized.

To characterize interactions between eCFP and eYFP a series of tandem repeats (CLYs) with various linker lengths were used for in vitro and in vivo measurements. In vitro measurements were taken three times over the course of a 10 month period with similar proximity ratios calculated each time. We attempted to recreate Evers et al. reported FRET values from 2006 with our data but failed to generate similar values using their formulas given. The methods from their paper was hard to follow and details were lacking. There are multiple ways to calculate FRET and we used a different formula after failing with their reported formula. The use of different approaches to calculate FRET may have contributed to different values.

In vivo measurements of the CLYs were carried out in CHO cells. The CLY proximity ratios were almost 4 times larger in vitro when compared to in vivo. However when comparing the trend of the proximity ratios to the hydrodynamic radii of the CLYs, they were similar. The hydrodynamic radii of the CLYs were calculated using the M_r obtained from SEC. Initial screening of the single FPs in different salt and pH conditions showed that the proteins were interacting with the column beads. In all conditions screened the elution volumes varied and were not consistent from run to run. The removal of the 6-his tag greatly affected CFP and future work should take the 6-his tag in consideration when determining the M_r. Different aliquots of single FPs were used for each screening condition. When the single FPs were run in the 100mM NaCl, 50mM HEPES buffer, pH 7.4 with the CLYs their elution volumes were different from when they were previously run during screening. Replicate samples of the single FP and CLY samples were run on the same day were similar if not exactly the same to each other. When running the SEC, standards should be run each time as elution volumes do vary from day to day. The inconsistently of SEC measurements from day to day shows that SEC may not be the best technique to determine the hydrodynamic radii of FP samples. In the future, different methods

including Fluorescent correlation spectroscopy and analytical ultracentrifugation should be used to determine the hydrodynamic radii of FPs. Ultimately, the use of the CLY data in vitro and in vivo will be used to create a universal reference ladder for in vivo FRET measurements. To create this ladder more CLYs with different linker lengths will be measured and characterized.

To investigate if a FP attached to the c-terminus end of a protein affects protein folding constructs referred to as PFPs was created with the SH3-GK domain of PSD-95 attached to eYFP. The chromophore of eYFP was knocked out so it would not fluoresce and interfere with smFRET measurements. Studies have shown that for PSD-95 to fold properly the SH3 domain must interact with the GK domain [24]. Previous measurements made in full length PSD-95 were compared to measurements made with PFPs [25]. Observed FRET efficiencies of PSD 1 and PFP 1 were 0.32 and 0.325 respectively for the 445-606 labeling sites. Observed FRET efficiencies of PSD 19 and PFP 2 were 0.782 and 0.743 respectively for the 445-702 labeling sites. The 445 labeling site in located in the SH3 domain and 606,702 are in the GK domain. Based on this data there is no apparent folding problems with the SH3-GK domain when eYFP is attached. The SH3-GK interaction is remains unaffected. It has been assumed that FPs attached to PSD-95 do not interfere with normal protein folding and the data presented here supports that assumption.

While eYFP does not interfere with the SH3-GK folding it may potentially interfere with normal protein functions. Green fluorescent protein and its variants are approximately 4.2-nm long with a 2.4-nm diameter barrel [4]. The formula weight of eYFP and SH3-GK domain are 30 and 36 kDa respectively. The massive size of eYFP may interfere with normal protein function, especially if eYFP not stationary. To see the relative location of eYFP when attached the SH3-GK domain, labeling pairs between eYFP and SH3-GK domain were used. Preliminary data

from PFP 3 suggests that eYFP may be changing conformations, by its large 0.36 Gaussian width. When calculating Föster's radius one parameter accounted for is κ^2, which is the rotation of dye. It is assumed that the κ^2 value is 2/3, meaning the dye is rotating freely in a cone shaped fashion. If the location of the labeling dyes on eYFP are in any way prevented from freely rotating then the κ^2.value must be corrected. This change in κ^2 value will change the values calculated by FRET.

To continue studying the location of eYFP relative to the SH3-GK domain of PSD-95 new PFP constructs with different labeling sites need to be measured to have a clearer idea of what is occurring. These new constructs have already been created, however growths show very low solubility with high levels of contaminants. The degree of solubility and contaminants varies from colony to colony grow suggesting that colonies should be screened before growths, to select the optimal colony. This also suggests that eYFP does not tolerate mutations very well. In an effort to increase solubility, the chromophore was reintroduced in those constructs, but solubility remained very low. The PFP 1 and 2 constructs show that eYFP can tolerate the chromophore knock out, but mutations on the beta sheets are not tolerated well. New studies are being conducted to determine which mutation sites eYFP can tolerate and then will be used to further study the location of eYFP relative to the SH3-GK domain of PSD-95.

Fluorescent proteins combined with FRET microscopy allow researchers to view protein-protein interactions and conformational changes in vivo. The use of fluorescent proteins can be problematic as demonstrated by the insolubility of eYFP with mutations attached to the SH3-GK domain of PSD-95. The interaction of the single FPs, CLYs and PFPs with column beads led to reduced protein yield and different M_r. However despite these difficulties the attachment of eYFP to the SH3-GK domain of PSD-95 did not affect the folding of the domains. The

differences of the CLY proximity ratios seen in vitro and in vivo show those measurements cannot be directly compared. The creation of an in vivo reference ladder will be a valuable tool to help interpret live cell FRET measurements in the future.

5. References

1. Lippincott-Schwartz, J. and G.H. Patterson, *Development and Use of Fluorescent Protein Markers in Living Cells.* Science, 2003. **300**(5616): p. 87-91.
2. Lorković, Z.J., J. Hilscher, and A. Barta, *Use of Fluorescent Protein Tags to Study Nuclear Organization of the Spliceosomal Machinery in Transiently Transformed Living Plant Cells.* Molecular Biology of the Cell, 2004. **15**(7): p. 3233-3243.
3. Shimomura, O., F.H. Johnson, and Y. Saiga, *Extraction, Purification and Properties of Aequorin, a Bioluminescent Protein from the Luminous Hydromedusan, Aequorea.* Journal of Cellular and Comparative Physiology, 1962. **59**(3): p. 223-239.
4. Ormö, M., et al., *Crystal Structure of the Aequorea victoria Green Fluorescent Protein.* Science, 1996. **273**(5280): p. 1392-1395.
5. Elsliger, M.-A., et al., *Structural and Spectral Response of Green Fluorescent Protein Variants to Changes in pH†,‡.* Biochemistry, 1999. **38**(17): p. 5296-5301.
6. Craggs, T.D., *Green fluorescent protein: structure, folding and chromophore maturation.* Chemical Society Reviews, 2009. **38**(10): p. 2865-2875.
7. Wachter, R.M., et al., *Structural basis of spectral shifts in the yellow-emission variants of green fluorescent protein.* Structure, 1998. **6**(10): p. 1267-1277.
8. Tsien, R.Y., *THE GREEN FLUORESCENT PROTEIN.* Annual Review of Biochemistry, 1998. **67**(1): p. 509-544.
9. Heim, R., D.C. Prasher, and R.Y. Tsien, *Wavelength mutations and posttranslational autoxidation of green fluorescent protein.* Proceedings of the National Academy of Sciences, 1994. **91**(26): p. 12501-12504.
10. Nagai, T., et al., *A variant of yellow fluorescent protein with fast and efficient maturation for cell-biological applications.* Nat Biotech, 2002. **20**(1): p. 87-90.
11. Patterson, G.H., et al., *Use of the green fluorescent protein and its mutants in quantitative fluorescence microscopy.* Biophys J, 1997. **73**(5): p. 2782-90.
12. Rekas, A., et al., *Crystal Structure of Venus, a Yellow Fluorescent Protein with Improved Maturation and Reduced Environmental Sensitivity.* Journal of Biological Chemistry, 2002. **277**(52): p. 50573-50578.
13. Stepanenko, O.V., et al., *Fluorescent proteins as biomarkers and biosensors: throwing color lights on molecular and cellular processes.* Curr Protein Pept Sci, 2008. **9**(4): p. 338-69.
14. Chudakov, D.M., et al., *Fluorescent proteins and their applications in imaging living cells and tissues.* Physiol Rev, 2010. **90**(3): p. 1103-63.

15. Sekar, R.B. and A. Periasamy, *Fluorescence resonance energy transfer (FRET) microscopy imaging of live cell protein localizations.* The Journal of Cell Biology, 2003. **160**(5): p. 629-633.
16. McCann, J.J., et al., *Optimizing methods to recover absolute FRET efficiency from immobilized single molecules.* Biophys J, 2010. **99**(3): p. 961-70.
17. Periasamy, A., *Fluorescence resonance energy transfer microscopy: a mini review.* Journal of Biomedical Optics, 2001. **6**(3): p. 287-291.
18. Broussard, J.A., et al., *Fluorescence resonance energy transfer microscopy as demonstrated by measuring the activation of the serine/threonine kinase Akt.* Nat. Protocols, 2013. **8**(2): p. 265-281.
19. Rizzo, M.A., et al., *Optimization of Pairings and Detection Conditions for Measurement of FRET between Cyan and Yellow Fluorescent Proteins.* Microscopy and Microanalysis, 2006. **12**(03): p. 238-254.
20. Piston, D.W. and G.-J. Kremers, *Fluorescent protein FRET: the good, the bad and the ugly.* Trends in Biochemical Sciences, 2007. **32**(9): p. 407-414.
21. Kim, E. and M. Sheng, *PDZ domain proteins of synapses.* Nat Rev Neurosci, 2004. **5**(10): p. 771-81.
22. El-Husseini, A.E.-D., et al., *Polarized Targeting of Peripheral Membrane Proteins in Neurons.* Journal of Biological Chemistry, 2001. **276**(48): p. 44984-44992.
23. Arnold, D.B. and D.E. Clapham, *Molecular determinants for subcellular localization of PSD-95 with an interacting K+ channel.* Neuron, 1999. **23**(1): p. 149-57.
24. McGee, A.W. and D.S. Bredt, *Identification of an Intramolecular Interaction between the SH3 and Guanylate Kinase Domains of PSD-95.* Journal of Biological Chemistry, 1999. **274**(25): p. 17431-17436.
25. McCann, J.J., et al., *Supertertiary structure of the synaptic MAGuK scaffold proteins is conserved.* Proceedings of the National Academy of Sciences, 2012. **109**(39): p. 15775-15780.
26. Evers, T.H., et al., *Quantitative understanding of the energy transfer between fluorescent proteins connected via flexible peptide linkers.* Biochemistry, 2006. **45**(44): p. 13183-92.
27. Choi, U.B., et al., *Modulating the Intrinsic Disorder in the Cytoplasmic Domain Alters the Biological Activity of the N-Methyl-d-aspartate-sensitive Glutamate Receptor.* Journal of Biological Chemistry, 2013. **288**(31): p. 22506-22515.
28. Craven, S.E., A.E. El-Husseini, and D.S. Bredt, *Synaptic Targeting of the Postsynaptic Density Protein PSD-95 Mediated by Lipid and Protein Motifs.* Neuron, 1999. **22**(3): p. 497-509.